

Exploring the Mechanism of Action and Survival and Immune Analysis of Lobotropin on Gastric Cancer through Network Pharmacology

Cao Xinyang^{1,2,a,*}, Zhan Hongju^{1,2,b,*}, Zhang Yu^{1,2,c}, Fang Quantang^{1,2,d}, Hong Bin^{1,2,e}, Sun Zijian^{1,2,f}

¹School of Chemical Engineering and Pharmacy, Jingchu Institute of Technology, 448000, Jingmen, China

²Hubei Key Laboratory of Drug Synthesis and Optimization, 448000, Jingmen, China

^a15030340312@xs.hnit.edu.cn, ^b2010102050026@whu.edu.cn, ^c2447277220@qq.com,

^d3272634034@qq.com, ^e2538453293@qq.com, ^f2669639201@qq.com

*Corresponding author

Abstract: With the help of DrugBank, TTD and SuperPred, the action targets of lobotropin were screened, and the action targets of gastric cancer were identified by DisGeNET, MalaCards and DigSee, and the two were taken to intersect, and there were 13 identical action targets, namely: HSP90AA1, NFKB1, MMP1, MMP2, OGG1, ABCC1, CXCR4, MTOR, ESR1, TLR4, AR, NFE2L2 and ITGB1, and the above genes were differentially expressed in gastric cancer by analysis of gastric cancer genes in the TCGA database. Drug-target-disease-pathway mapping, target interaction (PPI) network construction and KEGG and GO analysis of common targets screened five significant genes as NFKB1, TLR4, AR, MTOR and ITGB1, respectively. molecular docking was performed to show that lobeline had binding effect on all the above targets. Gene profiles of GSE14210, GSE15459, GSE22377, GSE29272, GSE51105 and GSE62254 were obtained from the GEO database plotting K-M survival curves indicated that NFKB1, TLR4, AR, MTOR and ITGB1 all had survival differences. Gastric cancer genes downloaded from the TCGA database were immunocorrelated by immunoassay for co-expression targets. The TIMER database was used to show the correlation of NFKB1, TLR4, AR, MTOR and ITGB1 on the direction of immune infiltration of gastric cancer cells. In conclusion lobotropin regulates NFKB1, TLR4, AR, MTOR and ITGB1 in gastric cancer tissues to achieve regulation of tumor progression.

Keywords: Stomach Cancer, Solanine, Immune infiltration of tumor cells, Molecular Docking

1. Introduction

Gastric cancer (STAD) is one of the most common cancers of the gastrointestinal tract worldwide [1][2]. Most patients can be cured with surgical resection. Patients with obvious early symptoms are usually diagnosed at an advanced stage, and more than half of patients present with metastases [3]. The remaining patients without advanced disease undergo surgery, but most are treated with chemotherapy and radiotherapy and eventually die from metastases. Therefore, in order to improve current radiotherapy, there is a growing interest in developing effective drugs that inhibit the proliferation of tumour cells and the ability of gastric cancer cells to metastasise.

In recent years in China, the proportion of people using Chinese medicine in the treatment of tumours has been increasing year on year, and it is thought that adjuvant Chinese medicine plus Western chemotherapy, radiotherapy and surgery as the main treatment is being accepted by more and more doctors and patients [4][5]. Glycoalkaloids (GA) are naturally occurring toxic compounds found in abundance in vegetables such as potatoes and plants, but after numerous experiments it has been shown that although glycoalkaloids are toxic to humans, they can be used to treat cancer by reducing the dose [6][7][8]. Lycopodium is a naturally occurring bioactive component and one of the major sterols found in lobelia and potato. Previous studies have shown that lycopodium acts as an inhibitor against a variety of cancers, inhibiting tumour cell growth by controlling mitosis and inducing tumour cell death [9][10]. In addition, some studies have shown that lycopene has anti-metastatic activity in various cancers [11][12][13][14][15]. Therefore, it is particularly important to identify potential lycopene for the treatment of STAD as well as potential molecular mechanisms and to explore pathway A regarding the relationship

between lycopene and gastric cancer.

2. Materials and methods

2.1. Screening for drug-disease co-target

With the help of DrugBank (<https://www.drugbank.ca>)^[16], TTD (<http://bidd.nus.edu.sg/group/ttd>)^[17] and SuperPred (<https://prediction.charite.de/>)^[18] for lobotropon. The drug targets were searched by UniProt, TTD and SuperPred. The drug-acting targets were translated into acting genes by UniProt (<https://www.uniprot.org/>)^[19]. Screening by DisGeNET (<http://www.disgenet.org/>)^[20], MalaCards (<http://www.disgenet.org/>)^[21] and DigSee (<http://210.107.182.61/geneSearch/>)^[22] for Disease genes. Combined with lobotropon action target genes gastric cancer genes were screened by jvenn (<http://www.bioinformatics.com.cn/>)^[23] for tumor-acting genes.

2.2. Expression of co-interacting genes in gastric cancer samples

RNAseq data (level3) and corresponding clinical information for the stomach were obtained from The Cancer Genome Atlas (TCGA) database (<https://portal.gdc.com>)^[24]. Analysis was performed using R v4.0.3. The common target of action will be referred to as target in the following.

2.3. Drug-target-disease-pathway mapping and target interaction (PPI) network construction

The screened target genes were uploaded into DAVID, and the top 10 corresponding pathways were screened by KEGG pathway analysis. The network topology parameters of drug-disease target-pathway and drug-shared target-pathway were analyzed using the built-in tools of Cytoscape 3.7.1 software^[25]. The obtained intersecting targets were then uploaded to STRING 11.0 platform to construct PPI network models: "homo sapiens" was selected as the biological species and "highest confidence" (>0.9) was selected as the minimum interaction threshold. ">0.9) to obtain the PPI network^[26].

2.4. Bioinformatics gene ontology (GO) analysis and Kyoto Encyclopedia of Genes and Genomes (KEGG) signaling pathway enrichment analysis

We used the KEGG rest API (<https://www.kegg.jp/kegg/rest/keggapi.html>) to obtain the latest KEGG Pathway gene annotations as background, mapped the genes to the background set, and used the R package clusterProfiler (version 3.14.3) for enrichment analysis to obtain the results of gene set enrichment^[27]. A minimum gene set of 5 and a maximum gene set of 5000 were set, and a P value of < 0.05 and a FDR of < 0.25 were considered statistically significant.

2.5. Molecular validation of key targets

In order to better elucidate the potential targets of lobotropon and specific protein binding activity in gastric cancer, the targets with the highest ranking in the "drug-target-disease-pathway" network were selected for molecular docking validation based on the above screened active ingredients and core targets, respectively. The crystal structures of the core target protein receptors were downloaded from the RCSB PDB database (<https://www.rcsb.org/>), and PyMoL software was used to remove the target protein receptor-independent ligands and non-protein molecules (e.g. water molecules); the chemical structures of the ligands were downloaded from the ZINC database (<http://zinc.docking.org/>). The chemical structure of the ligand was downloaded from ZINC database; the target protein receptor and ligand small molecules were pre-processed with AutoDock Tools, and the Grid Box was set up with the ligand as the center, and the docking active site was obtained with Autogrid module to obtain the binding energy. The components with the highest binding energy to the target protein were selected and the results were visualized using PyMoL software.^[28]

2.6. Survival analysis of key targets in gastric cancer samples

The gene expression datasets GSE14210, GSE15459, GSE22377, GSE29272, GSE51105 and GSE62254 were obtained from GEO, a free and publicly available database. The GSE14210, GSE15459, GSE22377, GSE29272, GSE51105 and GSE62254 datasets consisted of 640 samples; log rank was used to test the KM survival analysis comparing the survival differences between the two groups mentioned

above. For Kaplan-Meier curves, p values and hazard ratios (HR) with 95% confidence intervals (CI) were derived by logrank test and univariate Cox regression. The randomization threshold was set at 240 months and the bias component was excluded. All of the above analytical methods and R packages were performed using v4.0.3 version of R software (R Foundation for Statistical Computing, 2020).^[29]

2.7. Immunocorrelation analysis

RNAseq data (level3) and corresponding clinical information of gastric cancer tumors were obtained from The Cancer Genome Atlas (TCGA) database (<https://portal.gdc.com>). Single correlation maps were implemented by the R package ggstatsplot, and multi-gene correlation maps were presented by the R package pheatmap. Spearman's correlation analysis was used to describe correlations between quantitative variables without a normal distribution. A p-value less than 0.05 was considered statistically significant. All of the above analyses were implemented by R v4.0.3.^[30]

2.8. Immune infiltration analysis of tumor cells

The immune infiltration analysis of key genes in gastric cancer was uploaded in TIMER (<https://cistrome.shinyapps.io/timer/>). A p-value greater than 0.05 was considered statistically significant.^[31]

3. Conclusions

3.1. Screening of drug-disease co-targets and co-expression gene expression analysis

Combining DrugBank, TTD and SuperPred databases, a total of 130 genes corresponding to the action targets of lobotropins were identified. A total of 327 genes were found in gastric cancer tissues in DisGeNET, MalaCards and DigSee, including 13 co-expressed genes: HSP90AA1, NFKB1, MMP1, MMP2, OGG1, ABCC1, CXCR4, MTOR, ESR1, TLR4, AR, NFE2L2, and ITGB1 (Figure 1). In the TCGA database, visualization of the data after R language analysis indicated that HSP90AA1, NFKB1, MMP1, MMP2, ABCC1, CXCR4, MTOR, ESR1, TLR4, AR, NFE2L2 and ITGB1 were highly expressed and OGG1 and AR were lowly expressed in gastric cancer tissues (Figure 2).

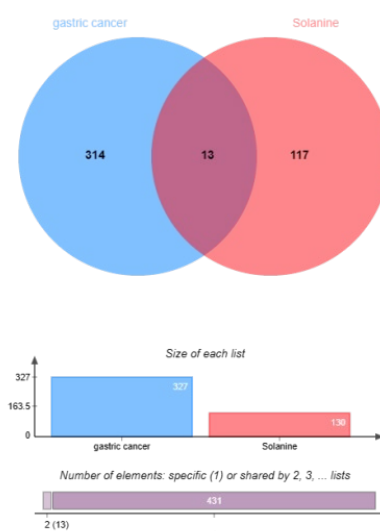


Figure 1: Genes corresponding to the action target of lobotropin intersect with gastric cancer genes. The blue area indicates a total of 327 significant genes for gastric cancer. The red area shows a total of 130 genes corresponding to the target of lobotropin action, and the purple area indicates a total of 13 co-expressed genes.

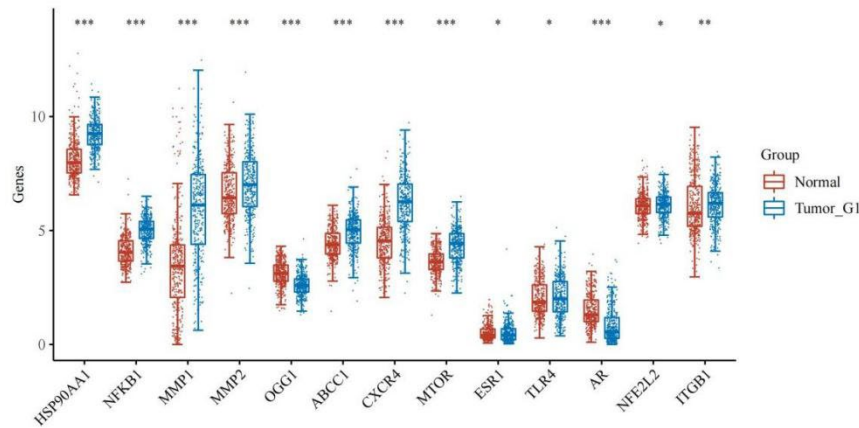


Figure 2: Gene expression distribution in tumor and normal tissues, where the horizontal coordinates represent different genes and the vertical coordinates represent the distribution of that related gene expression, where different colors represent different groups, $*p < 0.05$, $**p < 0.01$, $***p < 0.001$, and the asterisk represents the degree of significance ($*p$). Two groups of samples were significant by wilcox test, and two groups of samples were significant by Kruskal-Wallis test.

3.2. Drug-target-disease-pathway mapping and target point interaction (PPI)

The top ten cellular pathways swiped by the built-in KEGG pathway analysis in DAVID (Table 1), the cellular pathways, target genes, disease genes and drugs were imported into Cytoscape 3.7.1, resulting in the five most highly associated genes, NFKB1, TLR4, AR, MTOR and ITGB1, and the five most associated cellular pathways hsa05207 (Chemical carcinogenesis - receptor activation), hsa04151 (PI3K-Akt signaling pathway), hsa05215 (Prostate cancer), hsa05170 (Human The STRING 11.0 platform was used to construct PPI reciprocal networks expressing a total of six most highly associated NFKB1, TLR4, AR, MTOR, HSP90AB1 and ITGB1 genes. Combining the drug-target-disease-pathway and PPI results ranked NFKB1, TLR4, AR, MTOR and ITGB1 as the most critical genes (Figure 3-C).

Table 1: Top ten cellular pathways swiped by built-in KEGG pathway analysis in DAVID

Category	Term	Count	Genes
KEGG PATHWAY	hsa05207:Chemical carcinogenesis - receptor activation	5	AR,HSP90AA1,ESR1,NFKB1,MTOR
KEGG PATHWAY	hsa04151:PI3K-Akt signaling pathway	5	ITGB1,HSP90AA1,TLR4,NFKB1,MTOR
KEGG PATHWAY	hsa04659:Th17 cell differentiation	3	HSP90AA1,NFKB1,MTOR
KEGG PATHWAY	hsa04621:NOD-like receptor signaling pathway	3	HSP90AA1,TLR4,NFKB1
KEGG PATHWAY	hsa05132:Salmonella infection	3	HSP90AA1,TLR4,NFKB1
KEGG PATHWAY	hsa05215:Prostate cancer	4	AR,HSP90AA1,NFKB1,MTOR
KEGG PATHWAY	hsa05170:Human immunodeficiency virus 1 infection	4	CXCR4,TLR4,NFKB1,MTOR
KEGG PATHWAY	hsa05131:Shigellosis	4	ITGB1,TLR4,NFKB1,MTOR
KEGG PATHWAY	hsa05235:PD-L1 expression and PD-1 checkpoint pathway in cancer	3	TLR4,NFKB1,MTOR

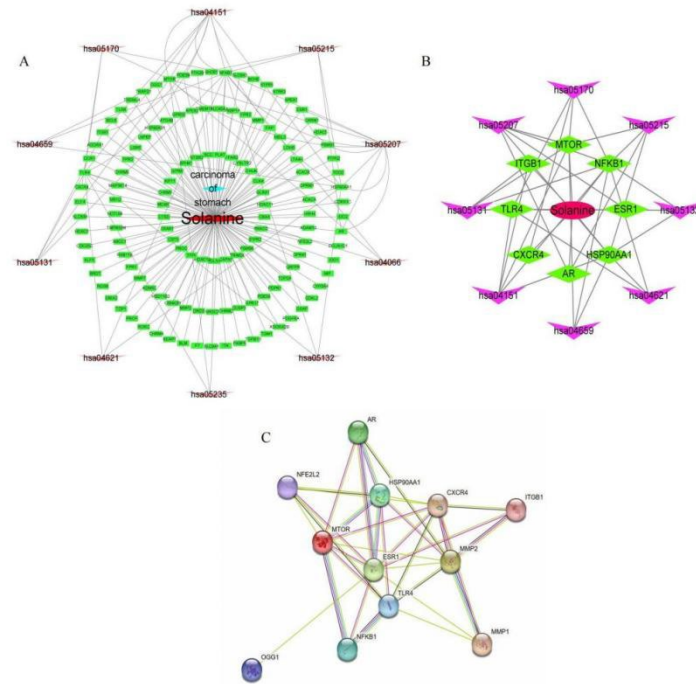
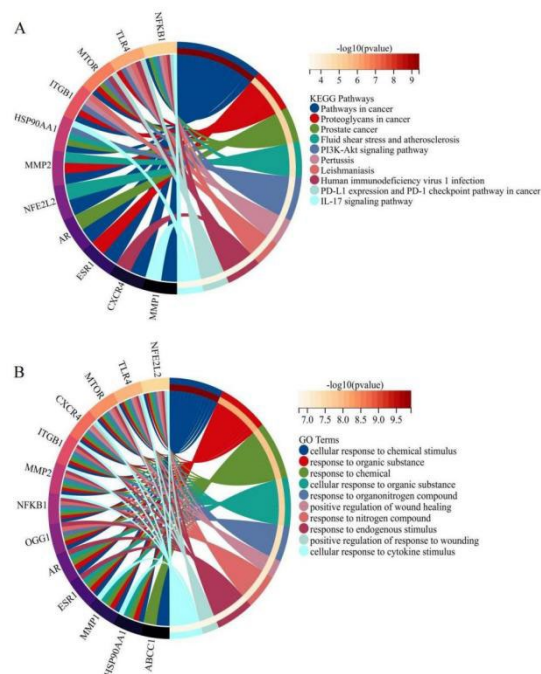


Figure 3: Drug-target-disease-pathway mapping and target-points interactions (PPI). (A) Drug-target-disease-pathway relationship interaction network. (B) PPI map of interactions based on shared genes. The lines represent the degree of interconnection, and the higher the degree of association, the stronger the effect.

3.3. Bioinformatics gene ontology (GO) analysis and Kyoto Encyclopedia of Genes and Genomes (KEGG) signaling pathway enrichment analysis



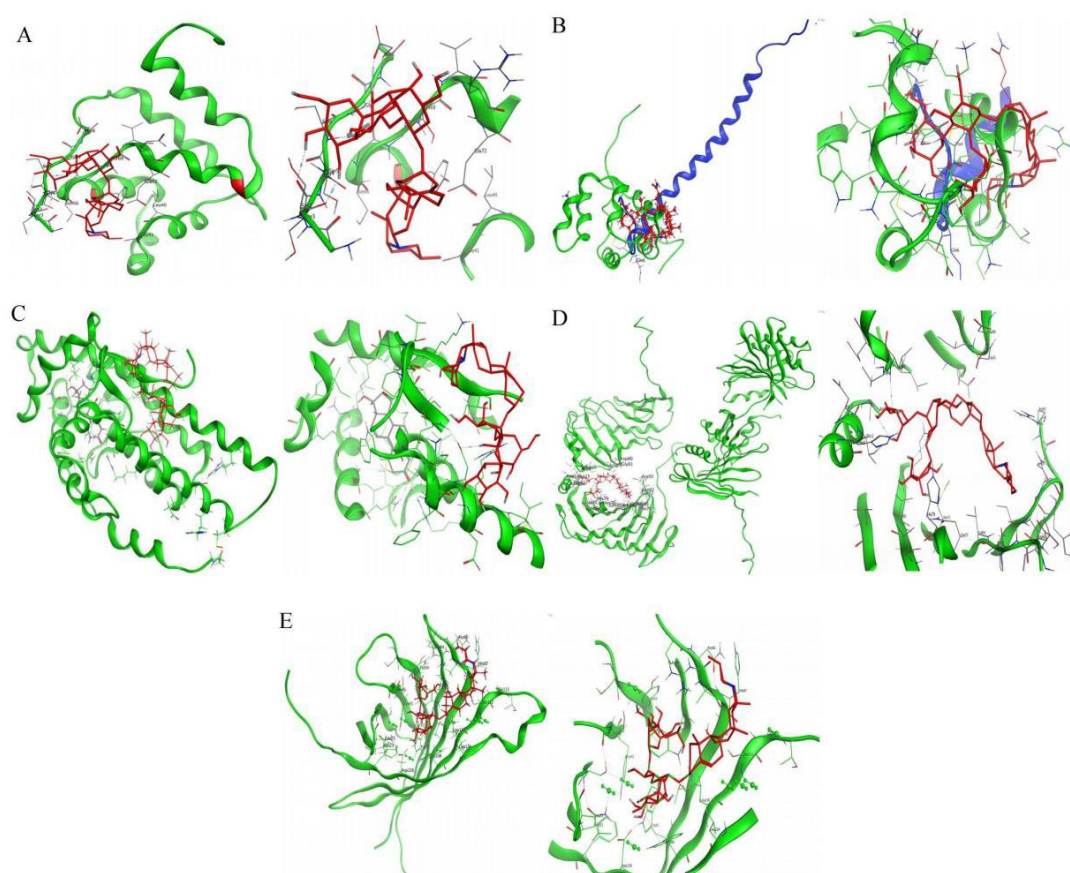
(A) KEGG analysis, a total of 10 pathways with the highest scores were screened and are indicated by symbols in the figure. (B) GO analysis, a total of 10 pathways with the highest scores were screened, which are indicated by symbols in the figure.

Figure 4: Bioinformatics gene ontology (GO) analysis and Kyoto Encyclopedia of Genes and Genomes (KEGG) signaling pathway enrichment analysis.

The targets were derived by KEGG analysis for pathways in cancer, proteoglycans in cancer, prostate cancer, fluid shear stress and atherosclerosis, PI3K- Akt signaling pathway, pertussis, leishmaniasis, human immunodeficiency virus 1 infection, PD-L1 expression in cancer and PD-1 checkpoint pathway and IL-17 signaling pathway, respectively. The GO analysis yielded that the targets responded to cellular responses to chemical stimuli, to organic substances, to chemical substances, to organic substances, to organonitrogen compounds, and to positive regulation of wounding. In summary, disease and drug common targets mainly target organic molecules and into gastric cancer cells, pathways in tumor itinerary, glycoproteins in tumor and PI3K- Akt signaling pathway for regulation. (Figure 4).

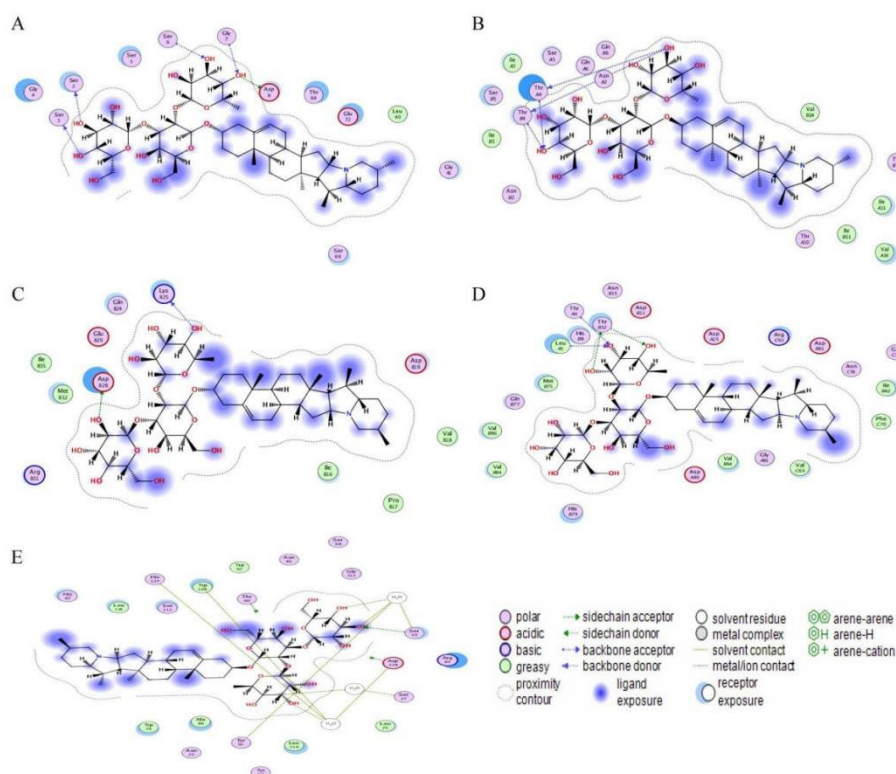
3.4. Molecular docking

Generally, the lower the binding energy of ligand and receptor, the more stable the binding conformation is. A binding energy <0 indicates that the ligand molecule can spontaneously bind to the receptor protein, and a binding energy ≤ -5 kJ/mol in natural molecules indicates that the ligand has good binding activity with the receptor. The binding energy of lobotropon to *NFKB1* was -7.3648 kJ/mol, *TLR4* was -6.4191 kJ/mol, *AR* was -6.5021 kJ/mol, *MTOR* was -8.8406 kJ/mol and *ITGB1* was -6.4191 kJ/mol. (Figure 5, 6).



(A) Molecular docking of lobomycin with *NFKB1*, the left panel shows the global picture of protein docking and the right panel shows the partial picture. (B) Molecular docking of lobin to *TLR4*, the left panel shows the global picture of protein docking and the right panel shows the local picture. (C) Docking of lobomycin with *AR* molecule, the left panel shows protein docking globally, the right panel shows locally. (D) Docking of lobomycin with *MTOR* molecule, the left panel shows the protein docking global, the right panel shows the partial panel. (E) Docking of lobin with *ITGB1* molecule, left panel shows protein docking global, right panel shows partial panel.

Figure 5: Molecular docking of lobomycin with *NFKB1*, *TLR4*, *AR*, *MTOR* and *ITGB1*.



(A) 2D plan view of the docking of lobin with NFKB1 molecule. (B) 2D plan view of the docking of lobin with TLR4 molecule. (C) 2D plan view of the docking of lobocalin with AR molecule. (D) 2D plan view of the docking of lobocalin with MTOR molecule. (E) 2D plan view of the docking of lobocalin with ITGB1 molecule.

Figure 6: 2D plan view of docking of lobomycin with NFKB1, TLR4, AR, MTOR and ITGB1 molecules.

3.5. Survival analysis of key targets

The gene profiles of GSE14210, GSE15459, GSE22377, GSE29272, GSE51105 and GSE62254 were obtained from the GEO database, and the survival curves of deviant components NFKB1, TLR4, AR, MTOR and ITGB1 were excluded to plot the K-M survival curves. Low expression of NFKB1, AR, MTOR and ITGB1 indicated a positive correlation with patient survival. high expression of TLR4 indicated a positive correlation with deep survival.(Figure 7).

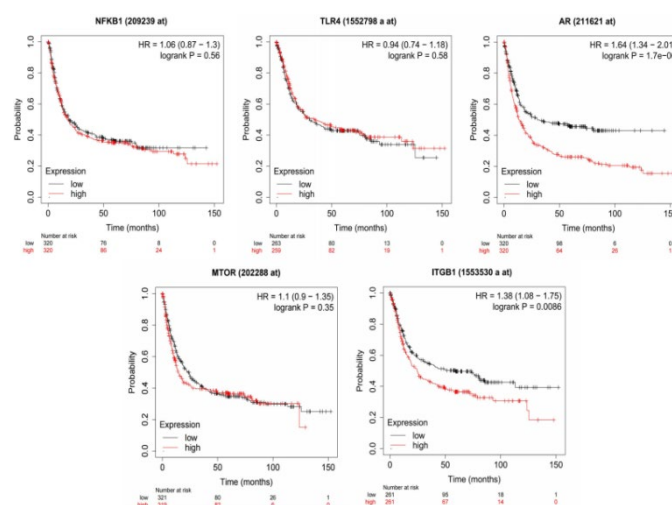


Figure 7: Survival curves of NFKB1, TLR4, AR, MTOR and ITGB1.

3.6. Immunocorrelation analysis

NFKB1, TLR4, AR, MTOR and ITGB1 showed correlation in immune correlation analysis with B cell, Endothelial cell, Macrophage, NK cell, T cell CD4+, T cell CD8+ and uncharacterized cell. Red color indicates positive correlation, blue color indicates negative correlation, the greater the color correlation. tlr4 positively correlated with uncharacterized cel, NFKB1 positively correlated with uncharacterized cel, MTOR positively correlated with NK cell, uncharacterized cell, ITGB1 positively correlated with B cell, uncharacterized cell. uncharacterized cell, and AR was positively correlated with uncharacterized cel.(Figure 8).

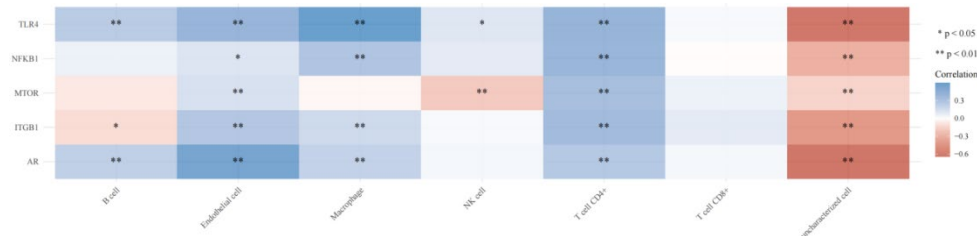


Figure 8: Multi-gene correlations: heat map of correlations between multiple genes or models and immune scores, both horizontal and vertical coordinates represent genes, where different colors represent correlation coefficients, darker colors represent stronger correlations between the two, * $p < 0.05$, ** $p < 0.01$, and asterisks represent the degree of importance (* p).

3.7. Immuno-infiltration analysis

NFKB1 was positively correlated in B Cell and Dendritic Cell and negatively correlated in CD8+ T Cell, CD4+ T Cell, Macrophage and Neutrophil cells. TLR4 was positively correlated in B Cell, CD4+ T Cell, Macrophage and Neutrophil and negatively correlated in Dendritic Cell. AR was positively correlated in B Cell, CD4+ T Cell, Macrophage, Dendritic Cell and Neutrophil. MTOR was positively correlated in B Cell, CD4+ T Cell, Macrophage, Dendritic Cell positive correlation, Neutrophil negative correlation. itgb1 positive correlation in B Cell, CD8+ T Cell, Macrophage, Dendritic Cell, CD4+ T Cell and Dendritic Cell Negative correlation.(Figure 9)

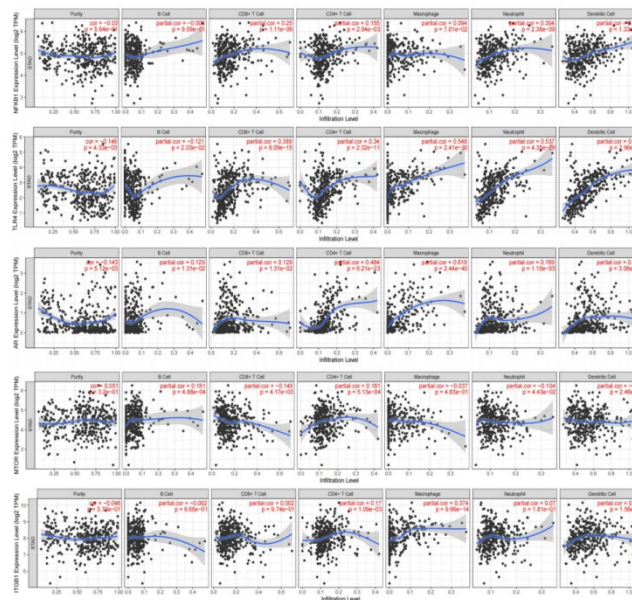


Figure 9: Immune infiltration analysis of NFKB1, TLR4, AR, MTOR and ITGB1 in gastric cancer tissues

4. Analysis of results

Thirteen genes were co-expressed during the analysis: HSP90AA1, NFKB1, MMP1, MMP2, OGG1,

ABCC1, CXCR4, MTOR, ESR1, TLR4, AR, NFE2L2 and ITGB1. In gastric cancer tissues, HSP90AA1, NFKB1, MMP1, MMP2, ABCC1, CXCR4, MTOR, ESR1, TLR4, AR, NFE2L2 and ITGB1 were highly expressed and OGG1 and AR were low expressed in gastric cancer tissues. The cellular pathways, target genes, disease genes and drugs were imported into Cytoscape 3.7. 1, resulting in the five most highly associated genes, NFKB1, TLR4, AR, MTOR and ITGB1, and the five most highly associated cellular pathways, hsa05207 (chemical carcinogenesis - receptor activation), hsa04151 (PI3K-Akt signalling pathway), hsa05215 (prostate cancer), hsa05170 (human immunodeficiency virus 1 infection) and hsa05131 (shigellosis). Gene ontology (GO) analysis and Kyoto Encyclopedia of Genes and Genomes (KEGG) pathway enrichment analysis yielded disease and drug common targets, mainly targeting organic molecules and becoming in gastric cancer cells, pathways in tumour itineraries, glycoproteins in tumours and PI3K-Akt signalling pathway for regulation.

Molecular docking showed that the binding energy of lobotropon to NFKB1 was -7.3648 kJ/mol, TLR4 was -6.4191 kJ/mol, AR was -6.5021 kJ/mol, MTOR was -8.8406 kJ/mol and ITGB1 was -6.4191 kJ/mol. /mol, which plays a critical role in the therapeutic treatment of gastric cancer cells.

Gene profiles of GSE14210, GSE15459, GSE22377, GSE29272, GSE51105 and GSE62254 were obtained from the GEO database NFKB1, AR, MTOR and ITGB1 low expression showed positive correlation with patient survival. High expression of TLR4 showed positive correlation with deep survival of patients. In the analysis with immune correlation, TLR4 was positively correlated with uncharacterised cel, NFKB1 was positively correlated with uncharacterised cel, MTOR was positively correlated with NK cell, uncharacterised cell, ITGB1 was positively correlated with B cell, uncharacterised cel positive correlation and AR positive correlation with uncharacterised cel. Immune infiltration of tumour cells was positively correlated with NFKB1 in B cells and dendritic cells and negatively correlated with CD8+ T cells, CD4+ T cells, macrophages and neutrophils. TLR4 was positively correlated with B cell, CD4+ T cell, macrophage and neutrophil in dendritic cell. AR was positively correlated with B cell, CD4+ T cell, macrophage, dendritic cell and neutrophil. MTOR was positively correlated with B cell, CD4+ T cell, macrophage, dendritic cell and neutrophil in dendritic cell. ITGB1 was positively correlated in B cell, CD8+ T cell, macrophage, dendritic cell and negatively correlated in CD4+ T cell and dendritic cell.

Acknowledgements

The authors thank the support of the Hubei Student Innovation and Entrepreneurship Foundation of China (S202211336029).

References

- [1] Gullo I, Grillo F, Mastracci L, Vanoli A, Carneiro F, Saragoni L, Limarzi F, Ferro J, Parente P, Fassan M. *Precancerous lesions of the stomach, gastric cancer and hereditary gastric cancer syndromes. Pathologica.* 2020 Sep;112(3):166-185.
- [2] Smyth EC, Nilsson M, Grabsch HI, van Grieken NC, Lordick F. *Gastric cancer. Lancet.* 2020 Aug 29;396(10251):635-648.
- [3] Thrift AP, El-Serag HB. *Burden of Gastric Cancer. Clin Gastroenterol Hepatol.* 2020 Mar;18(3):534-542.
- [4] Amashina T, Ishihara R, Nagai K, Matsuura N, Matsui F, Ito T, Fujii M, Yamamoto S, Hanaoka N, Takeuchi Y, Higashino K, Uedo N, Iishi H. *Long-term outcome and metastatic risk after endoscopic resection of superficial esophageal squamous cell carcinoma. Am J Gastroenterol.* 2013 Apr;108(4):544-51.
- [5] Leng JC, Gany F. *Traditional Chinese medicine use among Chinese immigrant cancer patients. J Cancer Educ.* 2014 Mar;29(1):56-61.
- [6] Gao Y, Yu AL, Li GT, Hai P, Li Y, Liu JK, Wang F. *Hexacyclic monoterpene indole alkaloids from Rauvolfia verticillata. Fitoterapia.* 2015 Dec;107:44-48.
- [7] Kuo CI, Chao CH and Lu MK: *Effects of auxins on the production of steroidal alkaloids in rapidly proliferating tissue and cell cultures of Solanum lyratum. Phytochem Anal.* 23:400-404. 2012.
- [8] Friedman M, Lee KR, Kim HJ, Lee IS and Kozukue N: *Anticarcinogenic effects of glycoalkaloids from potatoes against human cervical, liver, lymphoma and stomach cancer cells. J Agric Food Chem.* 53:6162-6169. 2005.
- [9] Yang SA, Paek SH, Kozukue N, Lee KR and Kim JA: *Alpha-chaconine, a potato glycoalkaloid, induces apoptosis of HT-29 human colon cancer cells through caspase-3 activation and inhibition of*

- ERK 1/2 phosphorylation. *Food Chem Toxicol.* 44:839–846. 2006.
- [10] Lee KR, Kozukue N, Han JS, Park JH, Chang EY, Baek EJ, Chang JS and Friedman M: Glycoalkaloids and metabolites inhibit the growth of human colon (HT29) and liver (HepG2) cancer cells. *J Agric Food Chem.* 52:2832–2839. 2004.
- [11] Lu MK, Shih YW, Chang Chien TT, Fang LH, Huang HC and Chen PS: α -Solanine inhibits human melanoma cell migration and invasion by reducing matrix metalloproteinase-2/9 activities. *Biol Pharm Bull.* 33:1685–1691. 2010.
- [12] Lv C, Kong H, Dong G, Liu L, Tong K, Sun H, Chen B, Zhang C, Zhou M. Antitumor efficacy of α -solanine against pancreatic cancer in vitro and in vivo. *PLoS One.* 2014 Feb 5;9(2):e87868.
- [13] Sun H, Lv C, Yang L, Wang Y, Zhang Q, Yu S, Kong H, Wang M, Xie J, Zhang C and Zhou M: Solanine induces mitochondria-mediated apoptosis in human pancreatic cancer cells. *Biomed Res Int.* 2014:8059262014.
- [14] Ji YB, Gao SY, Ji CF and Zou X: Induction of apoptosis in HepG2 cells by solanine and Bcl-2 protein. *J Ethnopharmacol.* 115:194–202. 2008.
- [15] Lu MK, Chen PH, Shih YW, Chang YT, Huang ET, Liu CR and Chen PS: Alpha-Chaconine inhibits angiogenesis in vitro by reducing matrix metalloproteinase-2. *Biol Pharm Bull.* 33:622–630. 2010.
- [16] Awale M, Reymond JL. Web-based 3D-visualization of the DrugBank chemical space. *J Cheminform.* 2016 May 4;8:25.
- [17] Zhang J, Liu X, Zhou W, Cheng G, Wu J, Guo S, Jia S, Liu Y, Li B, Zhang X, Wang M. A bioinformatics investigation into molecular mechanism of Yinzhihuang granules for treating hepatitis B by network pharmacology and molecular docking verification. *Sci Rep.* 2020 Jul 10;10(1):11448.
- [18] Nickel J, Gohlke BO, Erehman J, Banerjee P, Rong WW, Goede A, Dunkel M, Preissner R. SuperPred: update on drug classification and target prediction. *Nucleic Acids Res.* 2014 Jul;42(Web Server issue):W26-31.
- [19] UniProt Consortium. Reorganizing the protein space at the Universal Protein Resource (UniProt). *Nucleic Acids Res.* 2012 Jan;40(Database issue):D71-5.
- [20] Bauer-Mehren A, Rautschka M, Sanz F, Furlong LI. DisGeNET: a Cytoscape plugin to visualize, integrate, search and analyze gene-disease networks. *Bioinformatics.* 2010 Nov 15;26(22):2924-6.
- [21] Rappaport N, Fishilevich S, Nudel R, Twik M, Belinky F, Plaschkes I, Stein TI, Cohen D, Oz-Levi D, Safran M, Lancet D. Rational confederation of genes and diseases: NGS interpretation via GeneCards, MalaCards and VarElect. *Biomed Eng Online.* 2017 Aug 18; 16(Suppl 1):72.
- [22] Kim J, So S, Lee HJ, Park JC, Kim JJ, Lee H. DigSee: Disease gene search engine with evidence sentences (version cancer). *Nucleic Acids Res.* 2013 Jul; 41(Web Server issue):W510-7.
- [23] Bardou P, Mariette J, Escudié F, Djemiel C, Klopp C. jvenn: an interactive Venn diagram viewer. *BMC Bioinformatics.* 2014 Aug 29; 15(1):293.
- [24] Chandran UR, Medvedeva OP, Barmada MM, Blood PD, Chakka A, Luthra S, Ferreira A, Wong KF, Lee AV, Zhang Z, Budden R, Scott JR, Berndt A, Berg JM, Jacobson RS. TCGA Expedition: A Data Acquisition and Management System for TCGA Data. *PLoS One.* 2016 Oct 27; 11(10):e0165395.
- [25] Piñero J, Saúch J, Sanz F, Furlong LI. The DisGeNET cytoscape app: Exploring and visualizing disease genomics data. *Comput Struct Biotechnol J.* 2021 May 11; 19: 2960-2967.
- [26] Sharobeem S, Boulmier D, Leurent G, Bedossa M, Leclercq C, Mabo P, Martins RP, Tomasi J, Verhoye JP, Donal E, Sost G, Le Guellec M, Le Breton H, Auffret V. Prognostic impact of permanent pacemaker implantation after transcatheter aortic valve replacement. *Heart Rhythm.* 2022 July; 19(7):1124-1132.
- [27] Yuan F, Lu L, Zhang Y, Wang S, Cai YD. Data mining of the cancer-related lncRNAs GO terms and KEGG pathways by using mRMR method. *Math Biosci.* 2018 Oct; 304:1-8.
- [28] Luo Y, Chen P, Yang L, Duan X. Network pharmacology and molecular docking analysis on molecular targets and mechanisms of *Gastrodia elata* Blume in the treatment of ischemic stroke. *Exp Ther Med.* 2022 Nov 3;24(6):742.
- [29] Zheng Y, Tu J, Wang X, Yu Y, Li J, Jin Y, Wu J. The Therapeutic Effect of Melatonin on GC by Inducing Cell Apoptosis and Autophagy Induced by Endoplasmic Reticulum Stress. *Onco Targets Ther.* 2019 Nov 26;12:10187-10198.
- [30] Yang J, Gu W, Li Y. Biological enrichment prediction of polychlorinated biphenyls and novel molecular design based on 3D-QSAR/HQSAR associated with molecule docking. *Biosci Rep.* 2019 May 17;39(5):BSR20180409.
- [31] Yuan B, Liu G, Dai Z, Wang L, Lin B, Zhang J. CYP1B1: A Novel Molecular Biomarker Predicts Molecular Subtype, Tumor Microenvironment, and Immune Response in 33 Cancers. *Cancers (Basel).* 2022 Nov 17; 14(22):5641.